Performance Enhancement of Continuous-Phase Modulation Based OFDM Systems Using Chaotic Interleaving

EMAD S. HASSAN[1,2]

[1]Dept. of Electronics and Electrical Communications
Menoufia University
Faculty of Electronic Engineering, Menouf, 32952
EGYPT
emad.hassan@el-eng.menofia.edu.eg,

[2]Dept. of Electrical Engineering
Jazan University
Jazan
KSA.
eshassan@jazanu.edu.sa

Abstract: - In this paper, we propose a chaotic interleaving scheme for continuous-phase modulation based orthogonal frequency-division multiplexing (CPM-OFDM) systems. The idea of chaotic maps randomization (CMR) is exploited in this scheme. CMR generates permuted sequences from the sequences to be transmitted with lower correlation among their samples, and hence a better bit error rate (BER) performance can be achieved. The proposed CMR-CPM-OFDM system combines the advantages of frequency diversity and power efficiency from CPM-OFDM and performance improvement from chaotic interleaving. The BER performance of the CPM-OFDM system with and without chaotic interleaving is evaluated by computer simulations. Also, a comparison between chaotic interleaving and block interleaving is performed. Simulation results show that, the proposed chaotic interleaving scheme can greatly improve the performance of CPM-OFDM systems. Furthermore, the results show that the proposed chaotic interleaving scheme outperforms the traditional block interleaving scheme for CPM-OFDM systems. The results show also that, the proposed CMR-CPM-OFDM system provides a good trade-off between system performance and bandwidth efficiency.

Key-Words: - Chaotic interleaving, Frequency-Domain Equalization (FDE), Continuous-Phase Modulation (CPM), OFDM.

1 Introduction

The goal of future wireless communication systems is to support high-speed and high-quality multimedia transmission. However, there exist challenges for these systems such as the frequency selective channels, which are introduced by the multipath effect. OFDM is considered one of the most effective multicarrier transmission techniques for wireless communications, because it provides a large immunity to multipath fading and impulsive noise, and eliminates the need for complicated equalizers [1] – [6].

CPM is widely used in wireless communication systems [7]–[11], because of its constant envelope, which is required for efficient power transmission, and its ability to exploit the diversity of the multipath channel leading to an improvement in the BER performance. In [8] and [10], CPM has been applied in OFDM systems to solve the peak-to-average power ratio (PAPR) problem. In [12], a new low-complexity linear FDE approach for CPM systems was developed. Novel equalization algorithms in frequency domain for CPM systems are given in [13]. A CPM-SC-FDE structure for broadband wireless communication systems was proposed in [14]. The performance of OFDM and SC-FDE using CPM was studied in [15]. Although CPM systems have good performance and reasonable receiver complexity, they usually do not provide high bandwidth efficiency when compared with nonconstant-envelope modulation schemes such as Pulse Amplitude Modulation (PAM) and Quadrature Amplitude Modulation (QAM) [16].

Strong mechanisms for error reduction such as powerful error correction codes [17] and interleaving schemes [18] are required to reduce the channel effects on the data transmitted in the CPM-OFDM systems. Since the channel errors caused by the mobile wireless channels are bursty in nature, interleaving has become a must in wireless communication systems. Several interleaver schemes have been proposed. The simplest and most popular of such schemes is the block interleaver [18], [19]. In spite of the success of this scheme to achieve a good performance in wireless communication systems, there is a need for a much powerful scheme for severe channel degradation cases. Chaotic maps have been proposed for a wide range of applications in communications [20], and cryptography [21]–[24]. Due to the inherent strong randomization ability of

these maps, they can be used for data interleaving, efficiently.

In this paper, we propose a new interleaving scheme based on CMR for the CPM-OFDM system [25], [26]. The proposed scheme is based on the 2-D chaotic Baker map presented in [23], [24]. The idea of chaotic interleaving is to generate permuted sequences with lower correlation between their samples from the sequences to be transmitted. As a result, a better BER performance can be achieved. Moreover, it produces secure communication. It also enhances the bandwidth efficiency. The proposed CMR-CPM-OFDM system combines the advantages of frequency diversity and the power efficiency of CPM-OFDM system and the performance enhancement of CMR.

The rest of this paper is organized as follows. Section 2 presents the CPM-OFDM system model. The block interleaving and the proposed chaotic interleaving schemes are explained in section 3. The equalizer design and phase demodulator structure are explained in section 4 and 5, respectively. Section 6 discusses the bandwidth efficiency of CPM systems. Section 7 introduces the simulation results. Finally, Section 8 gives the concluding remarks.

2 CPM-OFDM System Model

The block diagram of the proposed CPM-OFDM system is shown in Fig. 1. A block length of K symbols is assumed with $X(k)$ (k = 0, 1, ...,K -1) representing the data sequence after symbol mapping and $x(n)$ (n = 0, 1,... ,N_{DFT} - 1) representing the N_{DFT} point IDFT of the data sequence $X(k)$. During each T-second symbol interval, the time samples $x(n)$ are subjected to a phase modulator (PM) step to get the constant envelope sequence, $s(n)$. This sequence is then interleaved to get $s_I(n)$ with the subscript I referring to the interleaving process. Then each data block is pre-appended with a cyclic prefix (CP) to mitigate the inter-block interference (IBI). The CP length must be longer than the channel impulse response. Finally, the continuous-time signal, $s_I(t)$ is generated at the output of the digital-to-analog (D/A) converter. According to [15], [27], $s_I(t)$ can be written as:

$$s(t) = Ae^{j\phi(t)} = Ae^{j[2\pi hx(t)+\theta]} \quad (1)$$

where A is the signal amplitude, h is the modulation index, θ is an arbitrary phase offset used to achieve CPM [8], and $x(t)$ is the real-valued message signal given by:

$$x(t) = C_n \sum_{k=1}^{K} I_k q_k(t) \quad (2)$$

where I_k are the M-ary real-valued data symbols, M is the number of constellation points, $q_k(t)$ are the orthogonal subcarriers, and C_n is a normalization constant. The real-valued data symbols, I_k, can be written as [15]:

$$I_k = \begin{cases} \Re\{X(k)\}, & k \le K/2 \\ -\Im\{X(k-K/2)\}, & k > K/2 \end{cases} \quad (3)$$

where $\Re\{X(k)\}$, $\Im\{X(k)\}$ are the real and the imaginary part of $\{X(k)\}$, respectively.

The transmitted signal $s_I(t)$ passes through the multipath channel. The channel impulse response is modelled as a wide-sense stationary uncorrelated scattering (WSSUS) process consisting of L discrete paths:

$$h(t) = \sum_{l=0}^{L-1} h(l)\delta(t-\tau_l) \quad (4)$$

where $h(l)$ and τ_l are the channel gain and delay of the lth path, respectively. The continuous-time received signal $r_I(t)$ can be expressed as:

$$r_I(t) = \sum_{l=0}^{L-1} h(l)s_I(t-\tau_l) + n(t) \quad (5)$$

where $n(t)$ is a complex additive white Gaussian noise (AWGN) with single-sided power spectral density N_0.

The output of the analog-to-digital (A/D) converter is sampled at $t = iT = (JK)$, where J is the oversampling factor then the CP is discarded. The ith (i = 0, 1,…, JK-1) sample of the received signal $r_I(t)$ is given by:

$$r_I(i) = \sum_{i=0}^{LJ-1} h(n)s(i-n) + n(i) \quad (6)$$

Defining $N_{DFT} = JK$, the received signal $r_I(i)$ is transformed into the frequency domain by using the N_{DFT}-point discrete Fourier transform (DFT). The received signal on the mth (m = 0, 1,…, N_{DFT} -1) subcarrier is given by:

$$R_I(m) = H(m)S_I(m) + N(m) \quad (7)$$

where R_I(m), H(m), S_I(m), and N(m) are the N_{DFT} - points DFT of $r_I(i)$, $h(i)$, $sI(i)$, and $n(i)$, respectively.

3 Interleaving Mechanisms

Error correction codes are usually used to protect signals through transmission over wireless channels. Most of the error correction codes are designed to correct random channel errors. However, channel errors caused by mobile wireless channels are bursty in nature. Interleaving is a process to rearrange the

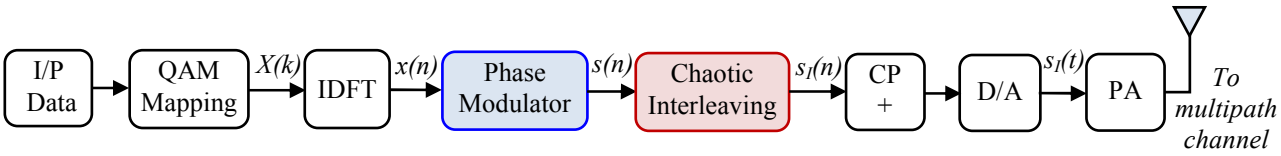

(a) Transmitter

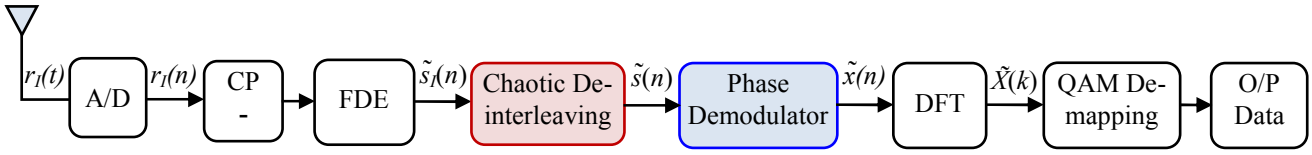

(b) Receiver

Figure 1: The CPM-OFDM system model with chaotic interleaving.

samples of the transmitted signal so as to spread bursts of errors over multiple code words.
The simplest and most popular of such interleavers is the block interleaver. We first review the basics of block interleaving [18]. Then we present the proposed chaotic interleaving mechanism in the next subsection.

3.1 The Block Interleaving Mechanism

The idea of block interleaving can be explained with the aid of Fig. 2. After PM, block interleaving is applied to the signal samples. The samples are first arranged to a matrix in a row-by-row manner and then read from this matrix in a column-by-column manner. Let us take a look at how the block interleaving mechanism can correct error bursts. Assume a burst of errors affecting four consecutive samples (1-D error burst) as shown in Fig. 2-b, with shades. After de-interleaving as shown in Fig. 2-c, the error burst is effectively spread among four different rows, resulting in a small effect for the 1-D error burst. With a single error correction capability, it is obvious that no decoding error will result from the presence of such 1-D error burst. This simple example demonstrates the effectiveness of the block interleaving mechanism in combating 1-D bursts of errors. Let us examine the performance of the block interleaving mechanism when a 2-D (2 × 2) error burst occurs [18], as shown in Fig. 2-b with shades. Figure 2-c indicates that this 2 × 2 error burst has not been spread, effectively, so that there are adjacent samples in error in the first and the second rows. As a result, this error burst cannot be corrected using a single error correction mechanism. That is, the block interleaving mechanism cannot combat the 2 × 2 bursts of errors.

3.2 The Proposed Chaotic Interleaving Mechanism

As mentioned in the previous subsection, the block interleaver is not efficient with 2-D bursts of errors. As a result, there is a need for advanced interleavers for this task. The 2-D chaotic Baker map in its discretized version is a good candidate for this purpose. After PM, the signal samples can be arranged into a 2-D format then randomized using the chaotic Baker map. The chaotic interleaver generates permuted sequences with lower correlation between their samples and adds a degree of encryption to the transmitted signal [25-26].

The discretized Baker map is an efficient tool to randomize the items in a square matrix. Let $B(n_1,\ldots,n_k)$, denote the discretized map, where the vector, $[n_1, \ldots, n_k]$, represents the secret key, S_{key}. Defining N as the number of data items in one row, the secret key is chosen such that each integer n_i divides N, and $n_1 + \ldots + n_k = N$. Let $N_i = n_1 + \ldots + n_i$. The data item at the indices (q, z), is moved to the indices [23], [25]:

$$B_{(n_1,\ldots,n_k)}(q,z) = \begin{pmatrix} \frac{N}{n_i}(q - N_i) + z \bmod \left(\frac{N}{n_i}\right), \\ \frac{n_i}{N}\left(z - z \bmod \left(\frac{N}{n_i}\right)\right) + N_i \end{pmatrix} \quad (8)$$

where $N_i \le q < N_i + n_i$, and $0 \le z < N$.
In steps, the chaotic permutation is performed as follows:

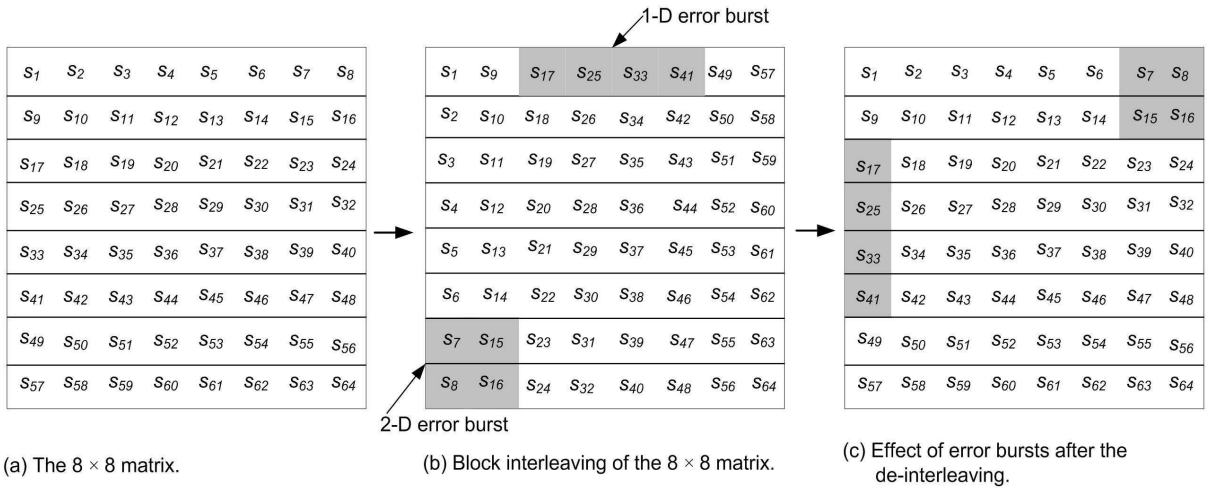

Figure 2: Block interleaving of an 8 × 8 matrix.

1) An $N \times N$ square matrix is divided into k rectangles of width n_i and number of elements N.
2) The elements in each rectangle are rearranged to a row in the permuted rectangle. Rectangles are taken from left to right beginning with upper rectangles then lower ones.
3) Inside each rectangle, the scan begins from the bottom left corner towards upper elements.

Figure 3 shows an example for the chaotic interleaving of an (8 × 8) square matrix (i.e. $N = 8$). The secret key, $S_{key} = [n_1, n_2, n_3] = [2, 4, 2]$. Note that, the chaotic interleaving mechanism has a better treatment to both 1-D and 2-D bursts of errors than the block interleaving. Errors are better distributed to samples after de-interleaving in the proposed chaotic interleaving mechanism. As a result, a better BER performance can be achieved with the proposed interleaving mechanism. Moreover, it adds a degree of security to the communication system. At the receiver of the proposed systems with chaotic interleaving, the received signal is then passed through an A/D converter, then the CP is discarded and the remaining samples are equalized as will be discussed in the next section to study the effect of the proposed chaotic interleaving scheme on the overall system performance.

4 Equalizer Design

In this section, the design of frequency domain equalizer is discussed. Also, we will define a new type of equalizer namely, regularized zero forcing (RZF) equalizer. As shown in Fig. 1, the received signals are equalized in the frequency domain. The equalized signals are then transferred back into the time domain by using an inverse DFT (IDFT).

Let $W(m)$, $(m = 0, 1, ..., N_{DFT} - 1)$, denote the equalizer coefficients for the *mth* subcarrier, the time domain equalized signal $\tilde{s}_I(i)$, which is the soft estimate of $s_I(i)$, can be expressed as follows:

$$\tilde{s}_I(i) = \frac{1}{N_{DFT}} \sum_{m=0}^{N_{DFT}-1} W(m) R_I(m) e^{j2\pi mi/N_{DFT}} \quad (9)$$

The equalizer coefficients $W(m)$ are selected to minimize the mean squared error between the equalized signal $\tilde{s}_I(n)$ and the original signal $s_I(n)$. The equalizer coefficients are computed according to a certain optimization rule leading to several types of equalizers such as:

- The zero-forcing (ZF) equalizer:

$$W(m) = \frac{1}{H(m)} \quad (10)$$

- The minimum mean square error (MMSE) equalizer:

$$W(m) = \frac{H^*(m)}{|H(m)|^2 + (E_b / N_0)^{-1}} \quad (11)$$

- The regularized zero forcing (RZF) equalizer:

$$W(m) = \frac{H^*(m)}{|H(m)|^2 + \beta} \quad (12)$$

where $(.)^*$ denotes the complex conjugate and β is the regularization parameter. The RZF equalizer described in (12) avoids the problems associated with the MMSE equalizer, such as the measurement of the signal power and the noise power, which are not

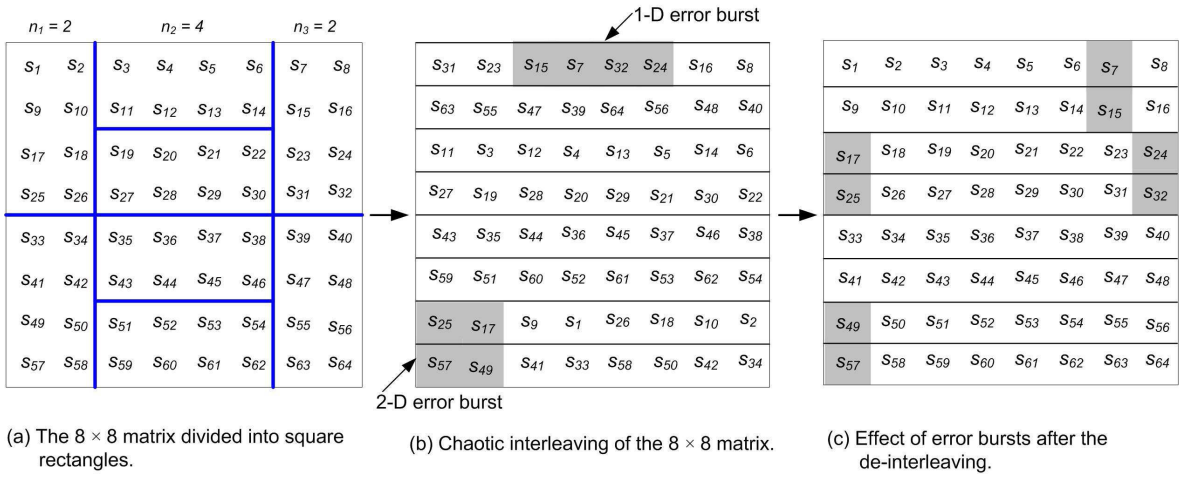

(a) The 8 × 8 matrix divided into square rectangles.

(b) Chaotic interleaving of the 8 × 8 matrix.

(c) Effect of error bursts after the de-interleaving.

Figure 3: Chaotic interleaving of an 8 × 8 matrix.

available prior to equalization. Moreover, the RZF equalizer avoids the noise enhancement caused by the ZF equalizer by introducing the regularization parameter β into the equalization process.

Considering the MMSE equalizer, the equalized signal can be expressed as:

$$\tilde{s}_I(i) = \underbrace{\frac{1}{N_{DFT}} \sum_{m=0}^{N_{DFT}-1} \frac{|H(m)|^2 S(m)}{|H(m)|^2 + (E_b/N_0)^{-1}} e^{j2\pi mi/N_{DFT}}}_{signal} + \underbrace{\frac{1}{N_{DFT}} \sum_{m=0}^{N_{DFT}-1} \frac{|H(m)|^* N(m)}{|H(m)|^2 + (E_b/N_0)^{-1}} e^{j2\pi mi/N_{DFT}}}_{noise} \quad (13)$$

The de-interleaving is then applied to the equalized samples. Afterwards, a phase demodulation step is applied to recover the data as explained in the next section.

5 Phase Demodulator

In this section, the design of the phase demodulator is discussed. Its block diagram is illustrated in Fig. 4. It starts with a finite impulse response (FIR) filter to remove the out-of-band noise. The filter is designed using the windowing technique [28]. The filter impulse response with a length L_f and a normalized cut-off frequency f_{nor} ($0 < f_{nor} \leq 1$), can be expressed as follows [25]:

$$g(n) = \frac{\sin\left(2\pi f_{nor}\left(n - \frac{L_f - 1}{2}\right)\right)}{\pi\left(n - \frac{L_f - 1}{2}\right)}, \quad 0 \leq n \leq L_f - 1 \quad (14)$$

In Eq. (14), if $n = (L_f - 1)/2$, $g(n) = 2\pi f_{nor}/\pi$. The output of FIR filter can be expressed as:

$$f(i) = \sum_{i=0}^{L_f - 1} g(n)\tilde{s}(i-n) \quad (15)$$

Afterwards, the phase of the filtered signal $f(i)$ is obtained:

$$\varphi(i) = \arg\big(f(i)\big) = \phi(i) + \delta(i) \quad (16)$$

where $\phi(i)$ denotes the phase of the desired signal, and $\delta(i)$ denotes the phase noise. Then, a phase unwrapper is used to minimize the effect of any phase ambiguities and to make the receiver insensitive to phase offsets caused by the channel nonlinearities.

Finally, the obtained signal is passed through a bank of K matched filters to get soft estimates of the data symbols $x(n)$ ($n = 0, \ldots, K - 1$).

6 Bandwidth Efficiency and Multipath Diversity of CPM Signals

The bandwidth efficiency is an important quality metric for a modulation format, since it quantifies how many information bits per second can be loaded per unity of the available bandwidth. To evaluate the bandwidth efficiency of a signal, its bandwidth needs to be estimated. Using Taylor expansion, the CPM

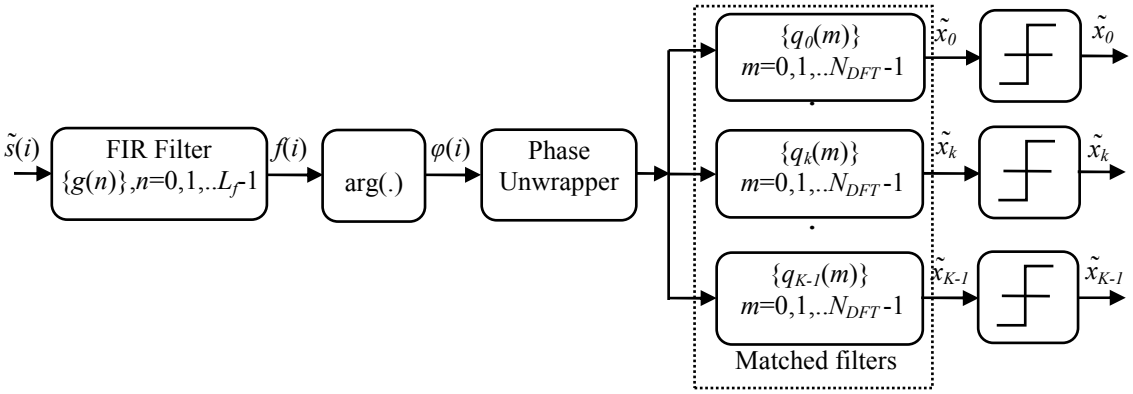

Figure 4: Phase demodulator.

signal described in Eq. (1), when $\theta = 0$, can be rewritten as:

$$s(t) = Ae^{j2\pi hx(t)} = A\sum_{n=0}^{\infty}\left[\frac{(j2\pi h)^n}{n!}\right]x^n(t)$$

$$= A\left[1 + j2\pi hx(t) - \frac{(2\pi h)^2}{2!}x^2(t) - j\frac{(2\pi h)^3}{3!}x^3(t) + \ldots\right] \quad (17)$$

The subcarriers are centered at the frequencies $\pm i/T$ Hz, $i = 1, 2, \ldots, K/2$. The effective double-side bandwidth of the message signal, $x(t)$, is defined as $W = K/T$ Hz. According to Eq.(17), the bandwidth of $s(t)$ is at least W, if the first two terms only of the summation are considered. Depending on the modulation index value, the effective bandwidth can be greater than W. A useful bandwidth expression for the CPM signal is the root-mean-square (RMS) bandwidth [29]:

$$\text{BW} = \max(2\pi h, 1)W \quad \text{Hz} \quad (18)$$

As shown in Eq. (18), the signal bandwidth grows with $2\pi h$, which in turn reduces the bandwidth efficiency. Since the bit rate is $R = K(\log_2 M)/T$ bps, the bandwidth efficiency of the CPM signal, η, can be expressed as:

$$\eta = \frac{R}{\text{BW}} = \frac{\log_2 M}{\max(2\pi h, 1)} \quad \text{bps/Hz} \quad (19)$$

The bandwidth efficiency of a CPM signal is controlled by two parameters, M and $2\pi h$. On the other hand, the bandwidth efficiency of an OFDM signal is $\log_2 M$, which depends only on M.

The Taylor expansion given in Eq. (17) reveals how a CPM signal exploits the frequency diversity in the channel for a large modulation index. This is not necessary the case, however. For a small modulation index, only the first two terms in Eq. (17) contribute:

$$s(t) \approx A\left[1 + j2\pi hm(t)\right] \quad (20)$$

In this case, the CPM signal does not have the frequency spreading given by the higher-order terms. Therefore, the CPM signal does not have the ability to exploit the frequency diversity of the channel [25].

7 Numerical Results and Discussion

In this section, simulation experiments are carried out to demonstrate the performance of the CPM-OFDM system and CPM-SC-FDE system when chaotic interleaving is applied in both systems. Another comparison study between the effect of using the proposed chaotic interleaving scheme and the traditional block interleaving scheme in both systems is also presented. 4-ary ($M = 4$) pulse amplitude modulation (PAM) data symbols are used in the simulations. Each block contains $K = 64$ symbols and each symbol is sampled 8 times ($J = 8$). A channel model following the exponential delay profile in [15] with a root mean square (RMS) delay spread $\tau_{rms} = 2$ μs is adopted except in Fig. 9. The channel is assumed to be perfectly known at the receiver. The SNR is defined as the average ratio between the received signal power and the noise power, which is given by SNR = A^2/N_0. The FIR filter has an impulse response length of $L_f = 11$ and a normalized cut-off frequency of $f_{nor} = 0.2$ [10], [30].

Figure 5 demonstrates the relation between the regularization parameter β and the BER for the

proposed CPM-OFDM system with chaotic interleaving at different SNR values. According to this figure, the best choice of β is 10^{-3}.

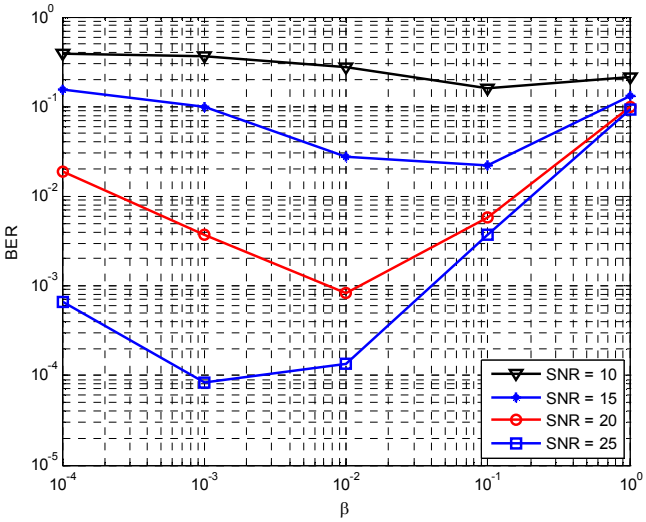

Figure 5: BER vs. the regularization parameter at different SNRs.

Figure 6 shows the BER performance of the proposed CPM-OFDM system with chaotic interleaving using ZF, RZF (with $\beta = 10^{-3}$), and MMSE frequency domain equalizers. The results show that, the MMSE equalizer outperforms both ZF and RZF. For example, at BER = 10^{-2}, MMSE outperforms RZF and ZF by 0.7 dB and 8 dB, respectively. On the other hand, the RZF avoids the problems associated with the MMSE such as the measurement of signal power and noise power which are not available prior to equalization with a slight degradation in SNR (0.7 dB). Moreover, the RZF avoids the noise enhancement caused by the ZF equalizer by the proper selection of regularization parameter β.

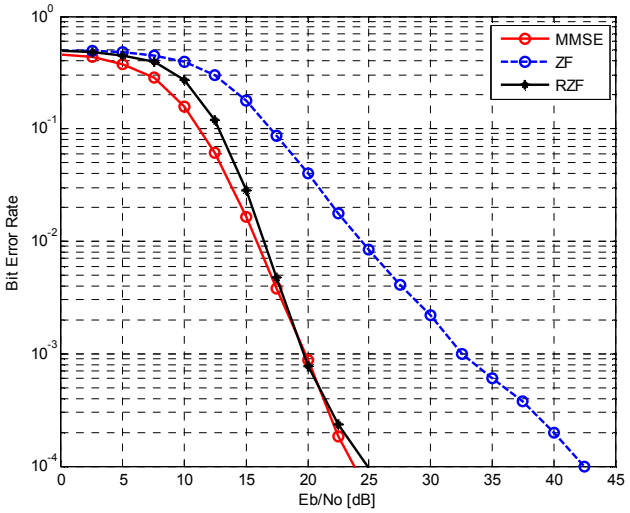

Figure 6: BER performance of CMR-CPM-OFDM system using ZF, RZF, and MMSE-FDEs.

Figure 7 shows the performance comparison between the proposed CPM-OFDM system with chaotic interleaving and the CPM-OFDM system described in [15] in terms of modulation index using MMSE equalizer. It is clear that, the proposed CPM-OFDM system outperforms the conventional CPM-OFDM system at a relatively small modulation index. So we can say that, the chaotic interleaving scheme improves the bandwidth efficiency when used with CPM-OFDM system.

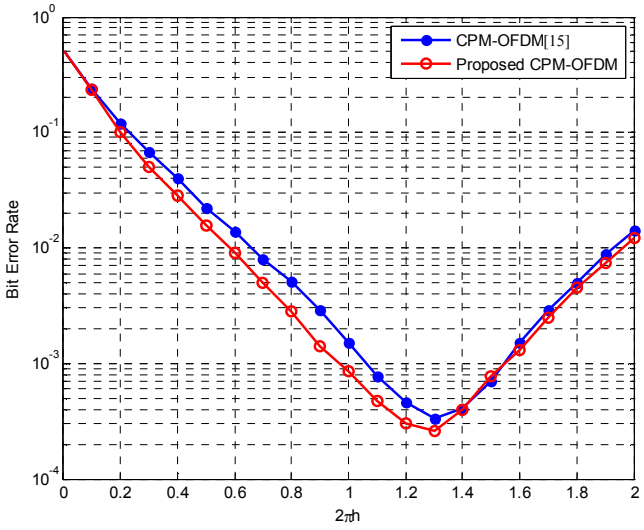

Figure 7: BER performance of the conventional CPM-OFDM and the proposed CPM-OFDM systems in terms of $2\pi h$ at SNR = 20 dB.

Table 1 shows the improvement percentage (**G**) in bandwidth efficiency of the proposed CPM-OFDM system, with chaotic interleaving over the conventional CPM-OFDM system [15]. For example, at BER of 3.2×10^{-4} and $M = 4$, the proposed CPM-OFDM system, needs $2\pi h = 1.17$ and according to Eq. (19), the bandwidth efficiency will be $\eta = 1.71$ *bps*. On the other hand, the conventional CPM-OFDM system needs $2\pi h = 1.3$, *i.e.* $\eta = 1.53$ *bps* which means that, the proposed CPM-OFDM system with chaotic interleaving can achieves about 12% improvements in bandwidth efficiency when compared to the conventional CPM-OFDM system.

Figure 8 shows a performance comparison between the conventional CPM-OFDM system no interleaving [15], the CPM-OFDM system with block interleaving, and the CPM-OFDM system with the proposed chaotic interleaving. It is clear that, the proposed CPM-OFDM system outperforms both the conventional CPM-OFDM and the CPM-OFDM with block interleaving. For example, at BER = 10^{-3}, the proposed CPM-OFDM system provides SNR improvements of 2.3 dB and 1.1 dB over the conventional CPM-OFDM system [15] and the CPM-OFDM system with block interleaving, respectively. This improvement is attributed to the strong randomization ability of the proposed chaotic interleaver.

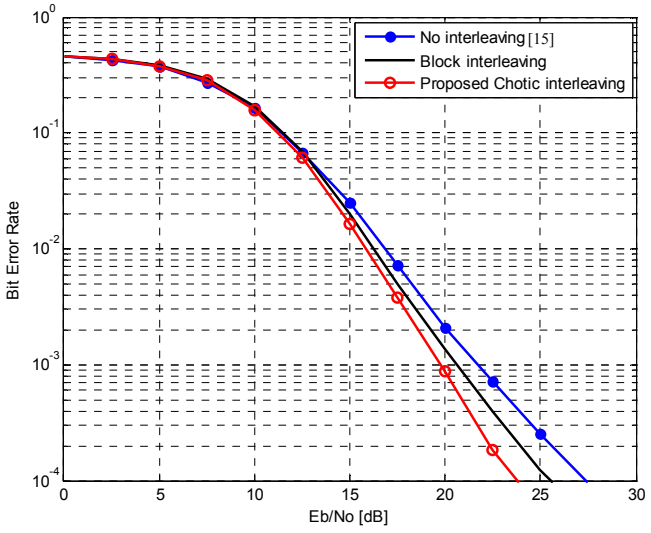

Figure 8: BER performance of CPM-OFDM no interleaving, with block interleaving, and with the proposed chaotic interleaving.

Table 1 Improvement percentage (**G**) in bandwidth efficiency in the CPM-OFDM system with and without chaotic interleaving.

BER	**CPM-OFDM (no interleaving)**	**CPM-OFDM (with chaotic interleaving)**	**G**
8×10^{-4}	$\eta = 1.818$ *bps* ($2\pi h = 1.1$)	$\eta = 2$ *bps* ($2\pi h = 1$)	10 %
3.2×10^{-4}	$\eta = 1.53$ *bps* ($2\pi h = 1.3$)	$\eta = 1.71$ *bps* ($2\pi h = 1.17$)	12 %

Figure 9 shows the performance of the conventional OFDM, the conventional CPM-OFDM [20], and the proposed CPM-OFDM systems in terms of a BER versus the normalized RMS delay spread, at a fixed SNR = 20 dB. In the flat fading case (*i.e.*, $\tau_{rms} = 0$), the performance of the conventional CPM-OFDM and the proposed CPM-OFDM systems converge with a small performance loss compared to the conventional OFDM system, due to the effect of the phase demodulator threshold. In frequency selective channels ($\tau_{rms} > 0$), however, the proposed CPM-OFDM system achieves a significant performance improvement over the other systems. It also provides a better performance than that in the flat fading case by achieving frequency diversity, especially at a high delay spreads.

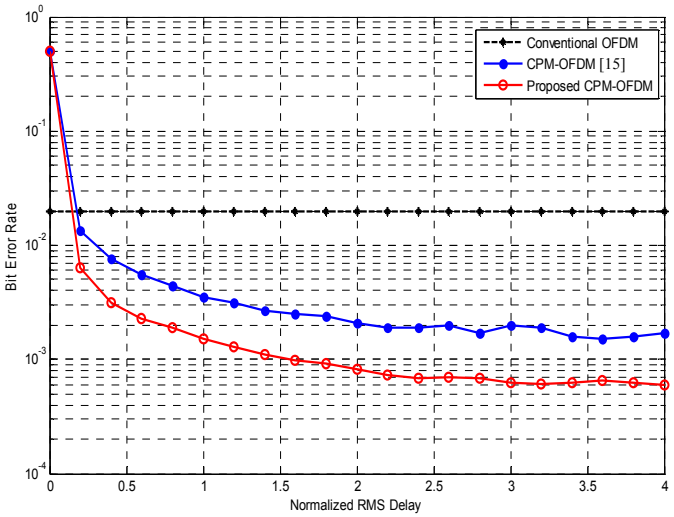

Figure 9: Effect of the RMS delay on the performance of the proposed CPM-OFDM, the conventional CPM-OFDM, and the conventional OFDM systems at an SNR = 20 dB.

8. Conclusions

An efficient chaotic interleaving scheme has been presented for the CPM-OFDM system. This scheme improves the BER performance of the CPM-OFDM system more effectively than the traditional block interleaving scheme, where it generates permuted sequences from the sequences to be transmitted with lower correlation between their samples. The performance of the proposed CMR-CPM-OFDM system was studied over a multipath fading channel with MMSE equalization. The obtained results revealed a noticeable performance improvement of the proposed CMR-CPM-OFDM system over the conventional OFDM and the CPM-OFDM systems, especially at high RMS delay spreads. It has been shown that, a moderate modulation index allows an efficient utilization of the channel frequency diversity, while maintaining high bandwidth efficiency.

References:

[1] R. V. Nee and R. Prasad, *OFDM for wireless multimedia communications*. Artech House, 2000.

[2] H. Schulze and C. Luders, *Theory and application of OFDM and CDMA wideband wireless communication*. John Wiley, 2005.

[3] P. Varzakas, "Optimization of an OFDM Rayleigh fading system", *International Journal of Communication Systems*, vol. 20, no.1, Jan. 2007, pp.1-7.

[4] H. Hou and G. Li, "Cross-layer packet dependent OFDM scheduling based on proportional fairness," *WSEAS Trans. on Commun.*, vol. 11, pp.1-15, Jan. 2012.

[5] S. Tseng, Y. Hsu, Y. Peng," Iterative multicarrier detector and LDPC decoder for OFDM systems," *WSEAS Trans. on Commun.*, vol. 11, pp. 124-134, March 2012.

[6] L. hoon, L. Jin, P. Sin-Chong, "VLSI Implementation for Interpolation-based Matrix Inversion for MIMO-OFDM Receivers" *Proc.s of the 6th WSEAS International Conference on Instrumentation, Measurement, Circuits & Systems*, 2007, pp. 24-27.

[7] J. Anderson, T. Aulin, and C. Sundeberg, *Digital phase modulation*. Plennum Press, New York, 1986.

[8] S. C. Thompson, A. U. Ahmed, J. G. Proakis, and J. R. Zeidler, "Constant envelope OFDM phase modulation: spectral containment, signal space properties and performance," in *IEEE Milcom, vol. 2, Monterey*, 2004, pp. 1129–1135.

[9] M. Kiviranta, A. Mammela, D. Cabric, D. A. Sobel, and R. W. Brodersen, "Constant envelope multicarrier modulation: performance evaluation in AWGN and fading channels," in *IEEE Milcom, vol. 2*, 2005, pp. 807–813.

[10] S. C. Thompson and A. U. Ahmed, "Constant-envelope OFDM," *IEEE Trans. Commun.*, vol. 56, no. 8, Aug. 2008.

[11] Y. Tsai, G. Zhang, and J.-L. Pan, "Orthogonal frequency division multiplexing with phase modulation and constant envelope design," in *IEEE Milcom, vol. 4*, 2005, pp. 2658–2664.

[12] W. Thillo, F. Horlin, J. Nsenga, V. Ramon, A. Bourdoux, and R. Lauwereins, "Low-complexity linear frequency domain equalization for continuous phase modulation," *IEEE Transactions on Wireless Commun.*, vol. 8, no. 3, 2009.

[13] F. Pancaldi and G. M. Vitetta, "Equalization algorithms in the frequency domain for continuous phase modulations," *IEEE Transactions on Commun.*, vol. 54, no. 4, 2006.

[14] E.S. Hassan, Xu Zhu, S.E. El-Khamy, M.I. Dessouky, S.A. El-Dolil, F.E. Abd El-Samie, "A continuous phase modulation single-carrier wireless system with frequency domain equalization", *Proc. of ICCES-09*, Cairo, Egypt, 14-16 Dec. 2009.

[15] E.S. Hassan, Xu Zhu, S.E. El-Khamy, M.I. Dessouky, S.A. El-Dolil, F.E. Abd El-Samie, "Performance evaluation of OFDM and single-carrier systems using frequency domain equalization and phase modulation", *Int. J. Commun. Syst.*, vol. 24, pp.1–13, 2011.

[16] A. Barbieri, D. Fertonani, and G. Colavolpe, "Spectrally efficient continuous phase modulations," *IEEE Transactions on Wireless Commun.*, vol. 8, no. 3, 2009.

[17] J. castello, D.J., J. Hagenauer, H. Imai, and S. Wicker, "Applications of error-control coding," *IEEE Transactions on Information Theory*, vol. 44, Oct. 1998.

[18] Y. Q. Shi, X. M. Zhang, Z.-C. Ni, and N. Ansari, "Interleaving for combating bursts of

errors," *IEEE Circuts and systems magazine*, vol. 4, First Quarter 2004.

[19] V. D. Nguyen and H. Kuchenbecker, "Block interleaving for soft decision viterbi decoding in ofdm systems," in *IEEE VTC*, 2001, pp. 470–474.

[20] B. Jovic and C. Unsworth, "Chaos-based multi-user time division multiplexing communication system," *IET Commun.*, vol. 1, no. 4, 2007.

[21] R. Matthews, "On the derivation of a chaotic encryption algorithm," *Cryptologia XIII*, vol. 1, 1989.

[22] K. S. Deffeyes, "Encryption system and method," *US Patent*, no. 5001754, March 1991.

[23] J. Fridrich, "Symmetric ciphers based on two-dimensional chaotic maps," *Int. Journal of Bifurcation and Chaos*, vol. 8, Oct. 1998.

[24] F. Han, X. Yu, and S. Han, "Improved baker map for image encryption," in *ISSCAA*, 2006, pp. 1273–1276.

[25] E.S. Hassan, S.E. El-Khamy, M.I. Dessouky, S.A. El-Dolil, F.E. Abd El-Samie, "New interleaving scheme for continuous phase modulation based OFDM systems using chaotic maps", *Proc. of WOCN-09*, Cairo, Egypt, 28–30 April 2009.

[26] E.S. Hassan, Xu Zhu, S.E. El-Khamy, M.I. Dessouky, S.A. El-Dolil, F.E. Abd El-Samie, "A chaotic interleaving scheme for continuous phase modulation based single-carrier frequency-domain equalization system", *Wireless Personal Commu.*, vol. 62, no. 1, pp.183-199, Jan., 2012.

[27] C.-C. Teng, J. Fonseka, and E. Dowling, "Non-coherent detectors for quadrature multiplexed continuous phase modulation signals," *IET Commun*, vol. 3, no. 4, 2009.

[28] J. G. Proakis and D. G. Manolakis, *Digital Signal Processing: Principles, Algorithms, and Applications, 3rd ed*. NJ: Prentice Hall, 1996.

[29] J. G. Proakis and M. Salehi, *Communication Systems Engineering*. New Jersey: Prentice Hall, 1994.

[30] V. N. Christofilakis, A. A. Alexandridis, K. P. Dangakis, P. Kostarakis, "Time Critical Parameters for Beamforming in Software Radios", *Recent Advances in Communications and Computer Science, Electrical and Computer Engineering Series*, pp. 30-36, 2003.